Monitoring autophagy in neural stem and progenitor cells

Romina L. Filippelli, Samaneh Kamyabiazar, and Natasha C. Chang*

Department of Biochemistry, Faculty of Medicine, McGill University, Montréal, Québec, Canada

* Correspondence:

Natasha C. Chang

natasha.chang@mcgill.ca

Running Head: Monitoring autophagy in NSCs

Abstract

Autophagy is a critical cellular program that is necessary for cellular survival and adaptation to nutrient and metabolic stress. In addition to homeostatic maintenance and adaptive response functions, autophagy also plays an active role during development and tissue regeneration. Within the neural system, autophagy is important for stem cell maintenance and the ability of neural stem cells to undergo self-renewal. Autophagy also contributes towards neurogenesis and provides the cells with sufficient energy to mediate cytoskeleton remodeling during the differentiation process. In differentiated neural cells, autophagy maintains neuronal homeostasis and viability by preventing the accumulation of toxic and pathological intracellular aggregates. However, prolonged autophagy or dysregulated upregulation of autophagy can result in autophagic cell death. Moreover, mutations or defects in autophagy that result in neural stem cell instability and cell death underlie many neurodegenerative diseases, such as Parkinson's. Thus, autophagy plays a multi-faceted role during neurogenesis from the stem cell to the differentiated neural cell. In this chapter, we describe methods to monitor autophagy at the protein and transcript level to evaluate alterations within the autophagy program in neural stem and progenitor cells. We describe immunoblotting and immunocytochemistry approaches for evaluating autophagy-dependent protein modifications as well as quantitative real-time PCR to assess transcript levels of autophagy genes. As autophagy is a dynamic process, we highlight the importance of using late-stage inhibitors to be able to assess autophagic flux and quantify the level of autophagy occurring within cells.

Keywords neural stem cell, autophagy, autophagic flux, nutrient deprivation, bafilomycin A1, chloroquine, LC3B immunoassay, p62/SQSTM1

1. Introduction

1.1 Autophagy: mechanisms and functions

Autophagy is a dynamic catabolic process fundamental to cell survival, as demonstrated by its remarkable conservation across eukaryotic species [1]. During autophagy, cytoplasmic material, i.e. macromolecules and organelles, are delivered to the lysosome for the purpose of degradation [2-4]. While the origin of these cytoplasmic entities may be exogenous, autophagy differs from vesicular trafficking in that it exclusively involves cellular materials that are accessible within the cytoplasm of the cell [4]. In order for an organism to grow and develop, a balance between synthesis and degradation is required; autophagy thus acts to maintain cellular homeostasis and plays roles in cellular remodeling due to its degradative nature [5].

In mammalian cells, three types of autophagy have been described, namely macroautophagy, microautophagy, and chaperone-mediated autophagy (CMA), each with their own distinct characteristics [6]. While all three types result in the delivery of intracellular cargo to the lysosome, CMA uses chaperones to identify and unfold autophagic substrates whereas microautophagy involves the use of lysosomal invaginations to capture cargo [7]. Contrastingly, in macroautophagy, hereafter referred to as autophagy, the intracellular cargo is sequestered away from the lysosome [7]. The first steps of autophagy (Fig. 1) involve the formation of a double membrane cup-shaped phagophore, also known as the isolation membrane [8]. The phagophore then expands to encapsulate cytoplasmic cargo and eventually fuses to form a complete vesicle known as the autophagosome [6, 8]. Autophagosomes can range in size depending on the cargo from 0.5-1.5 μm in diameter [6]. Formation of the autophagosome takes approximately 5-10 minutes and can be induced by a variety of stimuli, including nutrient starvation and rapamycin treatment, both of which suppress the mammalian target of rapamycin

complex 1 (mTORC1) pathway [8, 9]. Furthermore, the contents engulfed by the autophagosome can be both specific and non-specific [8]. Autophagosomes can fuse with endosomes or multivesicular bodies to form a structure known as the amphisome prior to delivering its contents to lysosomes [6]. Fusion of the autophagosome outer membrane with the lysosomal membrane results in the formation of an autolysosome [8]. Degradative hydrolases within the acidic lumen (pH 4.5-6) of the lysosome allow for degradation of the macromolecules and/or organelles previously sequestered by the autophagosome to their basic metabolic precursors (e.g. sugars, amino acids, and fatty acids) and are returned to the cytosol for reuse [6, 9].

Autophagy occurs under both basal and induced conditions, the former contributing to homeostatic constitutive turnover of cytosolic waste products and the latter serving mainly to acquire amino acids during periods of nutrient starvation [10, 11]. A basal level of autophagy serves to protect the cell by preventing autoactivation of inflammatory signals, enhancing lipophagy, and promoting the clearance of toxic cytosolic aggregates [12-16]. Autophagy levels can be upregulated by various triggers, such as starvation, to obtain nutrients to fulfill metabolic needs [17]. Other forms of stress that can activate autophagy include hypoxia, infection, growth factor deprivation and reactive oxygen species (ROS) accumulation [18]. While autophagy is generally considered a cell survival mechanism, prolonged autophagy or dysregulated upregulation of autophagy, for instance upon over-expression of the autophagy protein Beclin 1, can result in autophagic cell death [13, 19].

1.2 Role of autophagy in neural stem and progenitor cells

Autophagy plays a critical role in neural stem cells (NSCs) and their differentiated counterparts, which require a tightly regulated control of protein turnover [20]. During development,

multipotent NSCs that line the neural tube give rise to the central nervous system (CNS) by differentiating into the three major cell types of the CNS: neurons, astrocytes, and oligodendrocytes [21, 22]. Neurogenesis within the adult CNS, which involves the activation of quiescent NSCs towards differentiation, is limited to two regions within the telencephalon; the subventricular zone along the lateral ventricle, where migration of dividing neurons to the olfactory bulb has been observed, and the subgranular zone of the hippocampus, that is vital to the process of memory formation [23-26]. NSCs are thus responsible for postnatal generation of neuronal and glial cells, contributing to neurogenesis, neuroplasticity, and aging [18, 27, 28].

In NSCs, autophagy has been found to play critical roles in both self-renewal and differentiation (Fig. 2) [29]. Inactivation of the FOXO-family transcription factor members FOXO1, FOXO3, and FOXO4, which regulate transcriptional activation of autophagy, resulted in a depletion of NSCs and a decline in neurogenesis [30, 31]. Loss of NSC self-renewal in FOXO-depleted cells was attributed to an increase in ROS production [30]. Furthermore, cellular levels of ROS have been shown to drive NSC fate decisions, with increased ROS leading to the activation of NSC commitment and differentiation thereby inhibiting self-renewal [32]. Differentiation of NSCs is an energy-demanding process that requires extensive remodeling of the cytoskeleton [28]. Intriguingly, induction of autophagy in differentiating NSCs during both developmental and adult neurogenesis is necessary to provide sufficient energy required for this process [33, 34].

Differentiated neural cells are post-mitotic and are therefore unable to discard dysfunctional entities by cell division [35]. Thus, neural cells rely on the autophagy-lysosome pathway to degrade protein aggregates and damaged organelles [3, 35]. Genetic inactivation of the autophagy essential genes *Atg5* and *Atg7* result in an increase in neuronal ubiquitin-positive

aggregates, axonal swelling and subsequent retraction, as well as neuron cell death [3, 15, 35, 36]. In neurodegenerative diseases such as Parkinson's, Alzheimer's and Huntington's, defects in autophagy have been reported at different stages of the autophagic process [37]. For example, in Parkinson's, mutations in the genes encoding for PARK2 and PINK1, which selectively target damaged mitochondria for autophagy, result in the accumulation of dysfunctional mitochondria and induction of apoptosis [37]. NSCs and differentiated neural cells are thus particularly susceptible to changes in autophagy and are critically dependent on autophagy-mediated mechanisms for cellular homeostasis and viability.

1.3 Methods for monitoring autophagy

Here, we describe several methods for monitoring autophagy, and we present examples of data collected from these approaches using Neuro-2a (N2A) neuroblast cells. We present how to induce autophagy and inhibit autophagic flux *in vitro*, how to assess autophagy-dependent conversion of microtubule-associated protein 1 light chain 3 beta (MAP1LC3B, hereby referred to as LC3B) by immunoblotting and immunocytochemistry, how to assess degradation of the autophagy receptor p62/SQSTM1 by immunoblotting techniques, as well as how to evaluate autophagy by gene expression analysis using quantitative real-time PCR (RT-qPCR). In addition, we highlight the importance of evaluating autophagic flux using late-stage autophagy inhibitors and stress the need for performing complementary autophagy assays to ensure robustness of conclusions.

2. Materials

2.1 Measuring autophagic flux: LC3B lipidation and p62 degradation assays

2.1.1 Inducing autophagy in cells and inhibiting autophagic flux

1. Complete medium (CM): Dulbecco's Modified Eagle Medium (DMEM), 10% Fetal Bovine Serum (FBS), 1% Penicillin/Streptomycin
2. Earle's Balanced Salt Solution (EBSS)
3. 100 μM Bafilomycin A1 (Sigma-Aldrich), diluted in DMSO, *see* **Note 1**
4. 100 mM Chloroquine (Sigma-Aldrich), diluted in water, *see* **Note 1**

2.1.2 LC3B lipidation and p62 degradation immunoblotting assays

1. Lysis Buffer: 50 mM Tris-HCl pH 7.5, 150 mM NaCl, 1% Triton X-100, 0.1% SDS, 1 mM DTT, 1X protease inhibitor cocktail (Nacalai Tesque)
2. Bio-Rad Protein Assay Dye Reagent Concentrate (Bio-Rad)
3. 4X Laemmli Sample Buffer (Bio-Rad)
4. Resolving gel for SDS-PAGE: 0.375 M Tris-HCl, pH 8.8, 0.1% SDS, 15% acrylamide (for LC3B lipidation) or 10% acrylamide (for p62 degradation), 0.05% APS, 0.05% TEMED
5. Stacking gel for SDS-PAGE: 0.125 M Tris-HCl, pH 6.8, 0.1% SDS, 5% acrylamide, 0.1% APS, 0.1% TEMED
6. SDS-PAGE Running Buffer: 0.025 M Tris, 0.192 M Glycine, 0.1% SDS
7. Trans-Blot Turbo RTA Mini 0.45 μm LF PVDF Transfer Kit (Bio-Rad)
8. Washing solution: 1X PBS, 0.1% Tween (PBS-T)
9. Western Blot (WB) Blocking solution: PBS-T, 5% milk

10. Primary antibodies diluted in PBS-T, 5% BSA: LC3B (Cell Signaling Technology diluted at 1:1,000), p62/SQSTM1 (Sigma-Aldrich diluted at 1:1,000), GAPDH (AbLab Biologics diluted at 1:10,000)
11. Secondary antibodies diluted in WB Blocking Solution: Goat anti-Rabbit IgG (H+L) HRP Conjugate (Bio-Rad diluted at 1:5,000), Goat anti-Mouse IgG (H+L) HRP Conjugate (Bio-Rad diluted at 1:5,000)
12. Clarity Western ECL Substrate (Bio-Rad Laboratories)
13. HyBlot CL Autoradiography Film (Thomas Scientific)

2.1.3 Assessing p62 degradation by Simple Western

1. 12-230 kDa Jess Separation Module, 8 x 25 Capillary Cartridges (ProteinSimple)
2. Primary antibody diluted in Antibody Diluent 2 (ProteinSimple): p62/SQSTM1 (Sigma-Aldrich diluted at 1:300)
3. Secondary antibody: Goat anti-Rabbit Secondary HRP Antibody (ProteinSimple)

2.2 LC3B Immunofluorescence to detect autophagosomes

1. μ-Dish 35 mm, high ibiTreat (ibidi)
2. 8% Paraformaldehyde (PFA) aqueous solution (Electron Microscopy Sciences), diluted to 4% PFA in 1X PBS
3. Permeabilization solution: 1X PBS, 0.1 % Triton X-100, 0.1 M Glycine
4. Immunofluorescence (IF) blocking solution: 1X PBS, 5% donkey serum, 2% bovine serum albumin (BSA), 0.1% Triton X-100, 0.05% Tween

5. Primary antibody diluted in IF blocking solution: anti-LC3B (Cell Signaling Technology diluted at 1:100)
6. Washing solution: 1X PBS
7. Secondary antibody diluted in IF blocking solution: Donkey anti-Rabbit IgG (H+L) secondary antibody, Alexa Fluor 546 (Invitrogen diluted at 1:1,000)
8. ibidi Mounting Medium with DAPI (ibidi)

2.3 Transcriptional analysis of autophagy genes

1. TRIzol Reagent (Invitrogen)
2. Aurum Total RNA Mini Kit (Bio-Rad)
3. iScript Reverse Transcription Supermix (Bio-Rad)
4. SsoFast EvaGreen Supermix (Bio-Rad)
5. Primer sequences (*see* Table I)

3. Methods

3.1 Measuring autophagic flux: LC3B lipidation and p62 degradation assays

The conversion of the cytoplasmic protein LC3B during autophagy from LC3B-I to LC3B-II is a widely used assay to monitor the formation of autophagosomes [38]. During autophagy, LC3B-I is conjugated to phosphatidyl-ethanolamine to generate lipidated LC3B-II [39]. Upon lipidation, LC3B-II becomes integrated into the isolation membrane and the membrane of autophagosomes, thus making LC3B-II a reliable marker of autophagosomes [40, 41]. Due to the differential mobility of LC3B-I (16 kDa) and LC3B-II (14 kDa) by SDS-PAGE (i.e. LC3B-II migrating

faster than LC3B-I), the processing of LC3B can be resolved using a 15% polyacrylamide gel and visualized by immunoblotting with LC3B antibody.

Immunoblot analysis for the degradation of the autophagy receptor protein p62, which is also known as sequestome 1 (SQSTM1), is another method for monitoring autophagy [42]. p62 binds directly to LC3 and serves as an adapter protein through its ability to bind ubiquitinated proteins and target them for autophagic degradation within the lysosome [43]. Thus, p62 itself is degraded during autophagy and can be used as a readout for autophagic activity. Accordingly, in conditions where autophagy is inhibited, p62 protein levels accumulate [44].

3.1.1 Inducing autophagy in cells and inhibiting autophagic flux

Homeostatic autophagy occurs at a basal level and can be upregulated in response to nutrient deprivation. Due to the dynamic nature of the autophagic process, steady-state measurements of autophagy do not provide a complete picture of the actual level of autophagy occurring within the cell. For example, if steady-state LC3B-II protein levels are increased following a specific treatment, one cannot discriminate between the possibility that the treatment results in an augmentation in autophagy activity or in an impairment in autophagosome degradation [38]. Thus, the addition of autophagy inhibitors that block autophagic flux, such as bafilomycin A1 and chloroquine, prevents the turnover of autophagy-specific substrates, allowing for a quantifiable readout to compare the level of autophagic flux between different conditions.

While both bafilomycin A1 and chloroquine are commonly used inhibitors to block the late stages of autophagy, the two compounds differ in their mechanism of action. Bafilomycin A1 inhibits the vacuolar type H+-ATPase, thereby preventing autolysosome acidification and inhibits the activity of degradative lysosomal hydrolases. Bafilomycin A1 has also been shown to

inhibit autophagosome-lysosome fusion mediated by the sarco/endoplasmic reticulum calcium (SERCA)-ATPase [45]. Chloroquine, on the other hand, does not affect lysosomal acidity, and specifically blocks autophagic flux through the inhibition of autophagosome and lysosome fusion [46].

1. Conditions for assessing autophagic flux using bafilomycin A1 (BafA1). During autophagy induction, cells are maintained at 37 °C with 5% CO_2 for 2-4 h (*see* **Note 2**):
    a. Basal autophagy under normal growth conditions: Complete medium (CM) + DMSO (vehicle)
    b. Inhibiting basal autophagic flux in growth medium: CM + 100 nM BafA1 (1:1,000 dilution of a 100 μM working stock of BafA1)
    c. Induced autophagy during nutrient deprivation: EBSS + DMSO
    d. Inhibiting autophagic flux during nutrient deprivation: EBSS + 100 nM BafA1
2. Conditions for assessing autophagic flux using chloroquine (CQ) During autophagy induction, cells are maintained at 37 °C with 5% CO_2 for 2-4 h (*see* **Note 2**):
    a. Basal autophagy under normal growth conditions: Complete medium (CM) + H_2O (vehicle)
    b. Inhibiting basal autophagic flux in growth medium: CM + 100 μM CQ (1:1000 dilution of a 100 mM working stock of CQ)
    c. Induced autophagy during nutrient deprivation: EBSS + H_2O
    d. Inhibiting autophagic flux during nutrient deprivation: EBSS + 100 μM CQ

3.1.2 LC3B lipidation and p62 degradation immunoblotting assays

1. Collect cells following autophagy treatment as described in Section 3.1.1.
2. Lyse cells in lysis buffer (use a minimal lysis volume, *see* **Note 3**) on ice for 30 min.
3. Centrifuge cells at 13,000 × *g* at 4 °C for 10 min to remove cellular debris.
4. Determine protein concentration of cell lysates by Bradford assay using Bio-Rad protein assay dye reagent according to manufacturer's protocol.
5. Determine volume of lysate needed for 20 μg of protein for each LC3B lipidation and p62 degradation assay.
6. Add 5 μl of 4X Laemmli sample buffer to each 20 μg of protein and bring each sample up to a final volume of 20 μl. Denature the samples by incubating at 95 °C for 10 min.
7. Resolve denatured protein samples by SDS-PAGE; 15% acrylamide separation gel for LC3B lipidation and 10% acrylamide separation gel for p62 (*see* **Note 4**).
8. Transfer proteins from the gel to a PVDF membrane using the Trans-Blot Turbo Transfer System or other appropriate Western Blot apparatus.
9. Block membranes with Western Blot (WB) blocking solution for 1 h at room temperature.
10. Wash membranes 3 times 10 min with PBS-T.
11. Incubate with the appropriate primary antibody (anti-LC3B or anti-p62) diluted in PBS-T with 5% BSA (1:1,000 dilution) over-night at 4 °C.
12. Remove primary antibody solution (can be kept and re-used). Wash membranes 3 times 10 min with PBS-T.
13. Incubate with secondary antibody (anti-rabbit HRP) diluted in WB blocking solution (1:5,000 dilution) for 1 h at room temperature.
14. Wash membranes 4 times 10 min with PBS-T.

15. Detect proteins with ECL substrate and expose the membrane to autoradiography film.
16. Perform loading control detection by repeating steps 10-15 with anti-GAPDH primary antibody (1:10,000 dilution) followed by anti-mouse HRP secondary antibody (1:5,000 dilution).
17. Protein bands can be quantified by densitometric analysis using ImageJ software. Density of bands corresponding to LC3B and p62 should be normalized to the density of GAPDH (Fig. 1 and *see* **Notes 5 and 6**).

3.1.3 Assessing p62 degradation by Simple Western

In situations where protein sample yield is limited (i.e. when working with specific NSC populations), immunoassays can be performed using Simple Western technology, which allows for absolute quantitation of protein from as few as 25 cells [47]. We have optimized detection of p62 protein by Simple Western on a Jess instrument from a protein lysate concentration of 2 μg/μl and have obtained reliable quantification of p62 down to 0.2 μg/μl of lysate (*see* **Note 7**).

1. Follow steps 1-4 from Section 3.1.2.
2. Dilute protein lysates to a concentration of 2 μg/μl with 0.1X Sample Buffer (*see* **Note 8**).
3. Prepare Standard Pack Reagents (including DTT, Fluorescent 5X Master Mix, and Biotinylated Ladder) according to manufacturer's instructions.
4. Combine 1 part 5X Fluorescent Master Mix with 4 parts diluted protein lysates (2 μg/μl) and denature the samples by incubating at 95 °C for 10 min.

5. Follow the manufacturer's instructions for preparing the Jess 12-230 kDa Pre-filled Plate with Split Buffer, including:
    a. Denatured protein lysate with fluorescent protein standards (3 μl)
    b. Primary antibody (10 μl): rabbit anti-p62 (1:300 dilution in antibody diluent, *see* **Note 8**)
    c. Secondary conjugate (10 μl): anti-rabbit HRP (ready to use)
    d. Luminol-peroxide mix (15 μl) for chemiluminescence detection
6. Insert the capillary cartridge and assay plate into the Protein Simple Jess instrument and run the Simple Western assay through Compass software.

3.2 LC3B Immunofluorescence to detect autophagosomes

Performing an immunocytochemistry assay to visualize autophagosome formation serves as an excellent complementary assay to the LC3B lipidation and p62 degradation assays described above. When designing the experiment, it is important to consider the use of autophagic flux inhibitors to visualize autophagosome accumulation (*see* Fig. 4). LC3B immunostaining can be performed in combination with other proteins of interest to assess autophagosome colocalization. While the approach above allows for detection of endogenous LC3B incorporation into autophagosomes, ectopic expression of LC3B protein fused to a green fluorescent protein (GFP) tag (GFP-LC3B) is another commonly used method to visualize autophagosomes [48].

1. Seed cells onto μ-Dish 35 mm high ibiTreat dishes or sterilized glass cover slips suitable for fluorescence imaging.
2. Perform autophagy induction as in Section 3.1.1 when cells reach sufficient confluency.

3. Following autophagy induction, fix cells in 4% PFA for 10 minutes.
4. Wash cells 3 times 5 min with PBS. After the third wash, cells can be stored short-term (up to 2 weeks) in PBS at 4 °C until ready to perform immunocytochemistry.
5. Remove any remaining PBS and incubate cells with permeabilization solution for 10 min at room temperature.
6. Remove permeabilization solution and incubate cells in IF blocking solution for 1-2 h at room temperature.
7. Remove IF blocking solution and incubate with anti-rabbit LC3B primary antibody diluted (1:100) in IF blocking solution. Perform primary antibody incubation step over-night at 4 °C.
8. Remove primary antibody solution (can be stored and reused) and wash 3 times 10 min with PBS.
9. Incubate with donkey anti-rabbit Alexa 546 (or other appropriate secondary antibody conjugated with a fluorophore) diluted (1:1,000) in IF blocking solution. Perform incubation for 1 h and ensure that cells are protected from light to avoid fluorophore photobleaching (*see* **Note 9**).
10. Wash cells 3 times 10 min with PBS.
11. After removing the last PBS wash, add a few drops of ibidi mounting medium with DAPI to cover the surface of the cells. Store cells in the dark at room temperature over-night.
12. Cells are ready to be imaged by fluorescence microscopy. For long-term storage, immunostained cells can be kept at 4 °C.

3.3 Transcriptional analysis of autophagy genes

Autophagy is regulated at the level of transcription by several transcription factors, including the Transcription Factor EB (TFEB) and members of the Forkhead Box O1 (FOXO) family of transcription factors [49]. Thus, alterations in gene expression of autophagy genes can also be an indication of changes in the cellular autophagy status. We recommend examining a panel of autophagy genes (Table I) in combination with 2-3 reference genes (*see* **Note 10**) to obtain comprehensive and robust information regarding alterations in autophagy-related transcripts within the autophagic program.

1. Perform autophagy treatment on cells.
2. Collect the cells and perform RNA extraction using TRIzol reagent and RNA isolation using the Aurum Total RNA Mini Kit according to the manufacturers' instructions.
3. Perform final elution of RNA and determine RNA concentration. Isolated RNA may be stored at -80 °C.
4. Synthesize complementary DNA (cDNA) using the iScript Reverse Transcription Supermix according to the manufacturer's instructions. It is highly recommended to perform control cDNA synthesis reactions that include RNA but no reverse transcriptase enzyme (no RT, *see* **Note 11**).
5. Prepare reactions for RT-qPCR using SsoFast EvaGreen Supermix with cDNA and specific primers (*see* Table 1) according to manufacturer's instructions. For each primer pair, it is highly recommended to include no RT controls as well as no template controls (*see* **Note 11**).
6. Perform thermocycling with an appropriate real-time PCR instrument (ex: Bio-Rad CFX96 Touch Real-Time PCR Detection System). Thermocycling conditions: enzyme

activation 95 °C for 30 s, 40 cycles of denaturation at 95 °C for 5 s, annealing and extension at 59 °C for 5 s, followed by a melt curve of 65-95 °C in 0.5 °C increments for 5 s/step.

7. Analyze results and perform gene expression normalization to reference genes (*see* **Note 10**) using appropriate software (ex: CFX Maestro).

4. Notes

1. Bafilomycin A1 and chloroquine working stocks should be kept at -20 °C and aliquoted in small volumes to prevent multiple cycles of freeze/thaw. Chloroquine solutions should be kept protected from light.
2. 2 h of autophagy treatment with EBSS is sufficient to detect LC3B lipidation and p62 degradation. Cells can be maintained in EBSS for up to 4 h without a loss in cell viability.
3. When lysing cells, use a minimal volume of lysis buffer to avoid requiring large sample volumes for SDS-PAGE. The lysis volume will depend on the quantity of cells being lysed. An ideal protein lysate concentration is around 2 μg/μl.
4. Based on the apparent molecular weights of LC3B (14 kDa for LC3B-II and 16 kDa for LC3B-I) a 15% acrylamide gel is required to be able to resolve the lipidated and non-lipidated forms of LC3B. p62/SQSTM1 (62 kDa) is best visualized with a 10% acrylamide gel.
5. Care should be taken not to over-expose when using autoradiography film. Quantification of protein band density is accurate when protein bands are within the proper saturation

limit. Alternatively, chemiluminescence imaging systems such as the ChemiDoc (Bio-Rad) can be used.

6. Certain LC3B antibodies may have different affinities for LC3B-I and LC3B-II [35]. Conversion of LC3B during autophagic flux can be represented either as a comparison of total LC3B-II levels (the lipidated form), or as a ratio between the amount of LC3B-II to LC3B-I. Here, we quantified autophagic flux using both methods and obtained similar results (Fig. 3C and D).
7. We have performed Simple Western assays using anti-p62 (Sigma-Aldrich, P0067) and anti-LC3B (Cell Signaling Technology, 2775) antibodies. Results with the p62 antibody gave reliable results that complemented traditional immunoblotting (Fig. 3E and H). We obtained non-conclusive results with the anti-LC3B antibody and observed only a single LC3B peak in our analysis.
8. The optimal protein concentration and primary antibody dilution is dependent on the expression level of the protein of interest. Using a protein lysate concentration of 2 μg/μl, we have found that a 1:300 dilution of anti-p62 antibody is optimal.
9. Following the addition of the secondary antibody, care should be taken to avoid subjecting the cells to light.
10. We recommend using at least 2-3 reference genes to ensure that the transcript level of the reference genes are not impacted by the autophagy treatment. We have found that *Ppia* and *Rps18* reference genes are stable following EBSS treatment for 2 h and serve as reliable internal references. As a note of caution, we have found that *Gapdh* (a commonly used reference gene) levels are significantly reduced in nutrient deprivation (EBSS-treated) conditions compared to normal growth conditions.

11. When designing experiments for gene expression analysis, account for the need for biological and technical replicates (at least 3 of each) for RT-qPCR. In addition, to ensure quality of RT-qPCR experiments, no RT controls should be included to assess the amount of DNA contamination present in an RNA preparation, and no template controls should be included as a control for primer dimer formation and exogenous nucleic acid contamination in the reagents.

Acknowledgements

We thank Dr. Arezu Jahani-Asl for kindly providing N2A cells. R.F. is a recipient of a Maysie MacSporran Graduate Studentship from McGill University and supported by a Canada Graduate Scholarships Master's award from the Canadian Institutes of Health Research. Work in N.C.C.'s laboratory is supported by research grants from Jesse's Journey, Canadian Institutes of Health Research, Stem Cell Network, and a John R. Evans Leaders Fund from the Canada Foundation for Innovation. Figures 1 and 2 were created with BioRender.com.

Table

Table 1. Sequences of primers used for RT-qPCR analysis of autophagy gene expression

Gene	Forward primer	Reverse primer
Atg9	CGAGGCTGGTAACTGGAATC	CCTGTCCACCTTGTTAACCA
Atg13	CCAGGCTCGACTTGGAGAAAA	AGATTTCCACACACATAGATCGC
Gabarapl1	GGACCACCCCTTCGAGTATC	CCTCTTATCCAGATCAGGGACC
Map1lc3b	CACTGCTCTGTCTTGTGTAGGTTG	TCGTTGTGCCTTTATTAGTGCATC
p62/Sqstm1	CCCAGTGTCTTGGCATTCTT	AGGGAAAGCAGAGGAAGCTC
Vps34	TGTCAGATGAGGAGGCTGTG	CCAGGCACGACGTAACTTCT
Ppia (Reference)	CACTGCCAAGACTGAATG	GTCGGAAATGGTGATCTTC
Rps18 (Reference)	AACGGTCTAGACAACAAGCTG	AGTGGTCTTGGTGTGCTGAC

Figure Captions

Figure 1. Schematic model of the autophagic process.

Constitutive autophagy occurs at a basal homeostatic level in cells. Autophagy can also be upregulated and induced by triggers, such as starvation. The cargo destined for degradation is captured by an isolation membrane (phagophore), which expands to enclose cellular constituents within the autophagosome. The autophagosome subsequently fuses with the lysosome (autolysosome) where the cargo is degraded by lysosomal enzymes. Ultimately, the macromolecules and/or organelles previously sequestered by the autophagosome are degraded to their basic metabolic precursors and are returned to the cytosol for reuse.

Figure 2. The role of autophagy in neuronal stem cell differentiation.

Autophagy serves numerous roles throughout the process of neuronal stem cell (NSC) differentiation (designated in green text). Upon activation of NSCs, autophagy functions to provide energy for NSC cytoskeleton remodeling. In differentiated neural cells (neurons, oligodendrocytes, and astrocytes) autophagy plays a protective role. Neurons are post-mitotic and thus are unable to eliminate dysfunctional entities through cell division. Autophagy ensures neuronal homeostasis and viability by preventing the accumulation of aggregates, whose presence has been linked to neurodegenerative diseases such as Parkinson's.

Figure 3. LC3B lipidation and p62 degradation assays to examine autophagic flux.

A) N2A cells were maintained in complete medium (CM) or subjected to nutrient deprivation with EBSS for 2 h. To assess autophagic flux, cells in nutrient replete and deprived conditions

were treated with autophagy inhibitors, 100 nM bafilomycin A1 (BafA1) or 100 μM chloroquine (CQ), or vehicle as a control (DMSO or water). Protein lysates were resolved by SDS-PAGE with a 15% acrylamide gel and immunoblot analysis was performed with anti-LC3B and GAPDH antibodies. **B)** N2A cells were treated as described in **A** and protein lysates were resolved by SDS-PAGE with a 10% acrylamide gel and immunoblot analysis was performed with anti-p62 and GAPDH antibodies. **C)** Densitometric quantification of LC3B-II expression from the immunoblot in **A**, which was normalized to GAPDH as a protein loading control. Graph depicts densitometry values relative to control (CM + vehicle). **D)** Densitometric quantification of LC3B lipidation from **A**, expressed as a ratio of LC3B-II to LC3B-I expression. Graph depicts ratios relative to control (CM + vehicle). **E)** Densitometric quantification of p62 expression from **B**, which was normalized to GAPDH as a protein loading control. Graph depicts densitometry values relative to control (CM + vehicle). **F)** N2A protein lysates at a concentration of 2 μg/μl from **A** were subjected to Simple Western analysis using Protein Simple Jess. Representative Simple Western quantitative electropherogram showing chemiluminence signal from the CM + DMSO sample. Peak corresponding to p62 is indicated and expression level is quantified as the area under the curve as determined by Compass software. **G)** Simple Western lane view of protein lysates as described in **A** and **F**. **H)** Graph representing relative p62 protein expression level normalized to control (CM + vehicle).

Figure 4. Immunofluorescence analysis of autophagosome formation.

N2A cells were maintained in complete medium (CM) or subjected to nutrient deprivation with EBSS for 2 h. To assess autophagic flux, nutrient deprived cells were also subjected to treatment with DMSO (vehicle control) or bafilomycin A1 (BafA1). Cells were immunostained with anti-

LC3B antibody (red) and nuclei were counterstained with DAPI (blue). Fluorescence microscopy was performed using a Zeiss Axio Observer Z1 equipped with an AxioCam MR3 camera. Scale bar represents 5 μm.

Figure 5. Transcriptional upregulation of autophagy genes during nutrient deprivation. N2A cells were maintained in complete medium (CM) or subjected to nutrient deprivation with EBSS for 2 h. Real-time qPCR was performed with primers (*see* Table 1) for the indicated genes and gene expression was normalized to *Ppia* and *Rps18*. Gene expression fold changes of EBSS-treated cells are shown relative to CM-treated cells (n = 3 biological replicates ± SEM).

5. References

1. King JS (2012) Autophagy across the eukaryotes: is S. cerevisiae the odd one out? Autophagy 8 (7):1159-1162. doi:10.4161/auto.20527

2. Das G, Shravage BV, Baehrecke EH (2012) Regulation and function of autophagy during cell survival and cell death. Cold Spring Harb Perspect Biol 4 (6). doi:10.1101/cshperspect.a008813

3. Kulkarni VV, Maday S (2018) Compartment-specific dynamics and functions of autophagy in neurons. Dev Neurobiol 78 (3):298-310. doi:10.1002/dneu.22562

4. Galluzzi L, Baehrecke EH, Ballabio A, Boya P, Bravo-San Pedro JM, Cecconi F, Choi AM, Chu CT, Codogno P, Colombo MI, Cuervo AM, Debnath J, Deretic V, Dikic I, Eskelinen EL, Fimia GM, Fulda S, Gewirtz DA, Green DR, Hansen M, Harper JW, Jaattela M, Johansen T, Juhasz G, Kimmelman AC, Kraft C, Ktistakis NT, Kumar S, Levine B, Lopez-Otin C, Madeo F, Martens S, Martinez J, Melendez A, Mizushima N, Munz C, Murphy LO, Penninger JM, Piacentini M, Reggiori F, Rubinsztein DC, Ryan KM, Santambrogio L, Scorrano L, Simon AK, Simon HU, Simonsen A, Tavernarakis N, Tooze SA, Yoshimori T, Yuan J, Yue Z, Zhong Q, Kroemer G (2017) Molecular definitions of autophagy and related processes. EMBO J 36 (13):1811-1836. doi:10.15252/embj.201796697

5. Klionsky DJ, Emr SD (2000) Autophagy as a regulated pathway of cellular degradation. Science 290 (5497):1717-1721. doi:10.1126/science.290.5497.1717

6. Mijaljica D, Prescott M, Devenish RJ (2012) The intriguing life of autophagosomes. Int J Mol Sci 13 (3):3618-3635. doi:10.3390/ijms13033618

7. Parzych KR, Klionsky DJ (2014) An overview of autophagy: morphology, mechanism, and regulation. Antioxid Redox Signal 20 (3):460-473. doi:10.1089/ars.2013.5371

8. Shibutani ST, Yoshimori T (2014) A current perspective of autophagosome biogenesis. Cell Res 24 (1):58-68. doi:10.1038/cr.2013.159

9. He C, Klionsky DJ (2009) Regulation mechanisms and signaling pathways of autophagy. Annu Rev Genet 43:67-93. doi:10.1146/annurev-genet-102808-114910

10. Mizushima N (2007) Autophagy: process and function. Genes Dev 21 (22):2861-2873. doi:10.1101/gad.1599207

11. Pattison JS, Osinska H, Robbins J (2011) Atg7 induces basal autophagy and rescues autophagic deficiency in CryABR120G cardiomyocytes. Circ Res 109 (2):151-160. doi:10.1161/CIRCRESAHA.110.237339

12. Into T, Horie T, Inomata M, Gohda J, Inoue JI, Murakami Y, Niida S (2017) Basal autophagy prevents autoactivation or enhancement of inflammatory signals by targeting monomeric MyD88. Sci Rep 7 (1):1009. doi:10.1038/s41598-017-01246-w

13. Mizushima N, Levine B, Cuervo AM, Klionsky DJ (2008) Autophagy fights disease through cellular self-digestion. Nature 451 (7182):1069-1075. doi:10.1038/nature06639

14. Singh R, Kaushik S, Wang Y, Xiang Y, Novak I, Komatsu M, Tanaka K, Cuervo AM, Czaja MJ (2009) Autophagy regulates lipid metabolism. Nature 458 (7242):1131-1135. doi:10.1038/nature07976

15. Hara T, Nakamura K, Matsui M, Yamamoto A, Nakahara Y, Suzuki-Migishima R, Yokoyama M, Mishima K, Saito I, Okano H, Mizushima N (2006) Suppression of basal autophagy in neural cells causes neurodegenerative disease in mice. Nature 441 (7095):885-889. doi:10.1038/nature04724

16. Zhang Y, Goldman S, Baerga R, Zhao Y, Komatsu M, Jin S (2009) Adipose-specific deletion of autophagy-related gene 7 (atg7) in mice reveals a role in adipogenesis. Proc Natl Acad Sci U S A 106 (47):19860-19865. doi:10.1073/pnas.0906048106

17. Scott RC, Schuldiner O, Neufeld TP (2004) Role and regulation of starvation-induced autophagy in the Drosophila fat body. Dev Cell 7 (2):167-178. doi:10.1016/j.devcel.2004.07.009

18. Casares-Crespo L, Calatayud-Baselga I, Garcia-Corzo L, Mira H (2018) On the Role of Basal Autophagy in Adult Neural Stem Cells and Neurogenesis. Front Cell Neurosci 12:339. doi:10.3389/fncel.2018.00339

19. Pattingre S, Tassa A, Qu X, Garuti R, Liang XH, Mizushima N, Packer M, Schneider MD, Levine B (2005) Bcl-2 antiapoptotic proteins inhibit Beclin 1-dependent autophagy. Cell 122 (6):927-939. doi:10.1016/j.cell.2005.07.002

20. Son JH, Shim JH, Kim KH, Ha JY, Han JY (2012) Neuronal autophagy and neurodegenerative diseases. Exp Mol Med 44 (2):89-98. doi:10.3858/emm.2012.44.2.031

21. Kriegstein A, Alvarez-Buylla A (2009) The glial nature of embryonic and adult neural stem cells. Annu Rev Neurosci 32:149-184. doi:10.1146/annurev.neuro.051508.135600

22. Okano H, Temple S (2009) Cell types to order: temporal specification of CNS stem cells. Curr Opin Neurobiol 19 (2):112-119. doi:10.1016/j.conb.2009.04.003

23. Ferreira LM, Floriddia EM, Quadrato G, Di Giovanni S (2012) Neural regeneration: lessons from regenerating and non-regenerating systems. Mol Neurobiol 46 (2):227-241. doi:10.1007/s12035-012-8290-9

24. Altman J (1969) Autoradiographic and histological studies of postnatal neurogenesis. IV. Cell proliferation and migration in the anterior forebrain, with special reference to persisting neurogenesis in the olfactory bulb. J Comp Neurol 137 (4):433-457. doi:10.1002/cne.901370404

25. Altman J, Das GD (1965) Autoradiographic and histological evidence of postnatal hippocampal neurogenesis in rats. J Comp Neurol 124 (3):319-335. doi:10.1002/cne.901240303

26. Eriksson PS, Perfilieva E, Bjork-Eriksson T, Alborn AM, Nordborg C, Peterson DA, Gage FH (1998) Neurogenesis in the adult human hippocampus. Nat Med 4 (11):1313-1317. doi:10.1038/3305

27. Zhao X, Moore DL (2018) Neural stem cells: developmental mechanisms and disease modeling. Cell Tissue Res 371 (1):1-6. doi:10.1007/s00441-017-2738-1

28. Chen X, He Y, Lu F (2018) Autophagy in Stem Cell Biology: A Perspective on Stem Cell Self-Renewal and Differentiation. Stem Cells Int 2018:9131397. doi:10.1155/2018/9131397

29. Chang NC (2020) Autophagy and Stem Cells: Self-Eating for Self-Renewal. Front Cell Dev Biol 8:138. doi:10.3389/fcell.2020.00138

30. Paik JH, Ding Z, Narurkar R, Ramkissoon S, Muller F, Kamoun WS, Chae SS, Zheng H, Ying H, Mahoney J, Hiller D, Jiang S, Protopopov A, Wong WH, Chin L, Ligon KL, DePinho RA (2009) FoxOs cooperatively regulate diverse pathways governing neural stem cell homeostasis. Cell Stem Cell 5 (5):540-553. doi:10.1016/j.stem.2009.09.013

31. Renault VM, Rafalski VA, Morgan AA, Salih DA, Brett JO, Webb AE, Villeda SA, Thekkat PU, Guillerey C, Denko NC, Palmer TD, Butte AJ, Brunet A (2009) FoxO3 regulates neural stem cell homeostasis. Cell Stem Cell 5 (5):527-539. doi:10.1016/j.stem.2009.09.014

32. Khacho M, Clark A, Svoboda DS, Azzi J, MacLaurin JG, Meghaizel C, Sesaki H, Lagace DC, Germain M, Harper ME, Park DS, Slack RS (2016) Mitochondrial Dynamics Impacts Stem Cell Identity and Fate Decisions by Regulating a Nuclear Transcriptional Program. Cell Stem Cell 19 (2):232-247. doi:10.1016/j.stem.2016.04.015

33. Vazquez P, Arroba AI, Cecconi F, de la Rosa EJ, Boya P, de Pablo F (2012) Atg5 and Ambra1 differentially modulate neurogenesis in neural stem cells. Autophagy 8 (2):187-199. doi:10.4161/auto.8.2.18535

34. Ha S, Jeong SH, Yi K, Chu JJ, Kim S, Kim EK, Yu SW (2019) Autophagy Mediates Astrogenesis in Adult Hippocampal Neural Stem Cells. Exp Neurobiol 28 (2):229-246. doi:10.5607/en.2019.28.2.229

35. Maday S (2016) Mechanisms of neuronal homeostasis: Autophagy in the axon. Brain Res 1649 (Pt B):143-150. doi:10.1016/j.brainres.2016.03.047

36. Komatsu M, Waguri S, Chiba T, Murata S, Iwata J, Tanida I, Ueno T, Koike M, Uchiyama Y, Kominami E, Tanaka K (2006) Loss of autophagy in the central nervous system causes neurodegeneration in mice. Nature 441 (7095):880-884. doi:10.1038/nature04723

37. Nixon RA (2013) The role of autophagy in neurodegenerative disease. Nat Med 19 (8):983-997. doi:10.1038/nm.3232

38. Mizushima N, Yoshimori T (2007) How to interpret LC3 immunoblotting. Autophagy 3 (6):542-545. doi:10.4161/auto.4600

39. Tanida I, Ueno T, Kominami E (2004) LC3 conjugation system in mammalian autophagy. Int J Biochem Cell Biol 36 (12):2503-2518. doi:10.1016/j.biocel.2004.05.009

40. Kabeya Y, Mizushima N, Ueno T, Yamamoto A, Kirisako T, Noda T, Kominami E, Ohsumi Y, Yoshimori T (2000) LC3, a mammalian homologue of yeast Apg8p, is localized in autophagosome membranes after processing. EMBO J 19 (21):5720-5728. doi:10.1093/emboj/19.21.5720

41. Kabeya Y, Mizushima N, Yamamoto A, Oshitani-Okamoto S, Ohsumi Y, Yoshimori T (2004) LC3, GABARAP and GATE16 localize to autophagosomal membrane depending on form-II formation. J Cell Sci 117 (Pt 13):2805-2812. doi:10.1242/jcs.01131

42. Bjorkoy G, Lamark T, Pankiv S, Overvatn A, Brech A, Johansen T (2009) Monitoring autophagic degradation of p62/SQSTM1. Methods Enzymol 452:181-197. doi:10.1016/S0076-6879(08)03612-4

43. Pankiv S, Clausen TH, Lamark T, Brech A, Bruun JA, Outzen H, Overvatn A, Bjorkoy G, Johansen T (2007) p62/SQSTM1 binds directly to Atg8/LC3 to facilitate degradation of ubiquitinated protein aggregates by autophagy. J Biol Chem 282 (33):24131-24145. doi:10.1074/jbc.M702824200

44. Bjorkoy G, Lamark T, Brech A, Outzen H, Perander M, Overvatn A, Stenmark H, Johansen T (2005) p62/SQSTM1 forms protein aggregates degraded by autophagy and has a protective effect on huntingtin-induced cell death. J Cell Biol 171 (4):603-614. doi:10.1083/jcb.200507002

45. Mauvezin C, Neufeld TP (2015) Bafilomycin A1 disrupts autophagic flux by inhibiting both V-ATPase-dependent acidification and Ca-P60A/SERCA-dependent autophagosome-lysosome fusion. Autophagy 11 (8):1437-1438. doi:10.1080/15548627.2015.1066957

46. Mauthe M, Orhon I, Rocchi C, Zhou X, Luhr M, Hijlkema KJ, Coppes RP, Engedal N, Mari M, Reggiori F (2018) Chloroquine inhibits autophagic flux by decreasing autophagosome-lysosome fusion. Autophagy 14 (8):1435-1455. doi:10.1080/15548627.2018.1474314

47. Chen JQ, Heldman MR, Herrmann MA, Kedei N, Woo W, Blumberg PM, Goldsmith PK (2013) Absolute quantitation of endogenous proteins with precision and accuracy using a capillary Western system. Anal Biochem 442 (1):97-103. doi:10.1016/j.ab.2013.07.022

48. Mizushima N, Yoshimori T, Levine B (2010) Methods in mammalian autophagy research. Cell 140 (3):313-326. doi:10.1016/j.cell.2010.01.028

49. Fullgrabe J, Ghislat G, Cho DH, Rubinsztein DC (2016) Transcriptional regulation of mammalian autophagy at a glance. J Cell Sci 129 (16):3059-3066. doi:10.1242/jcs.188920

Figure 1

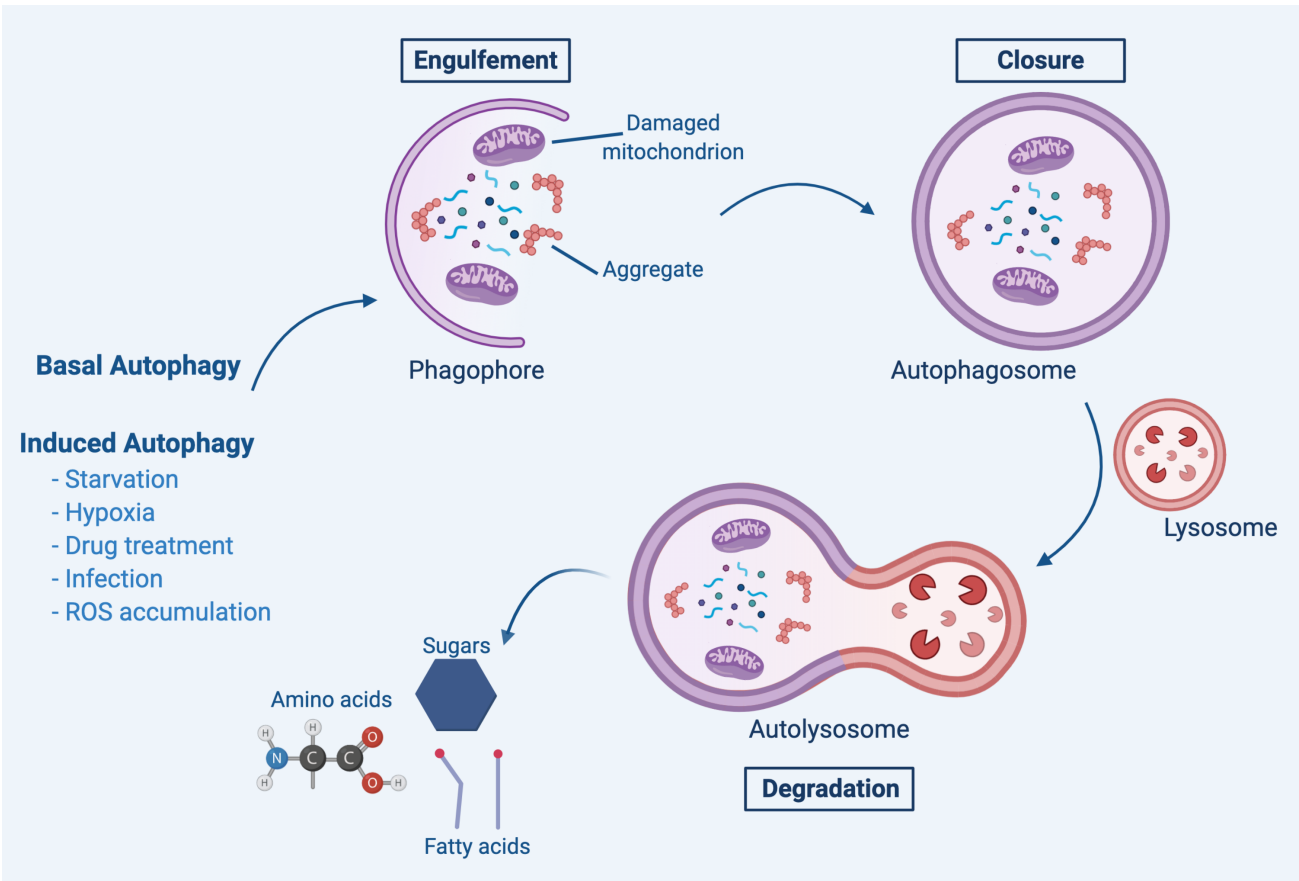

Figure 2

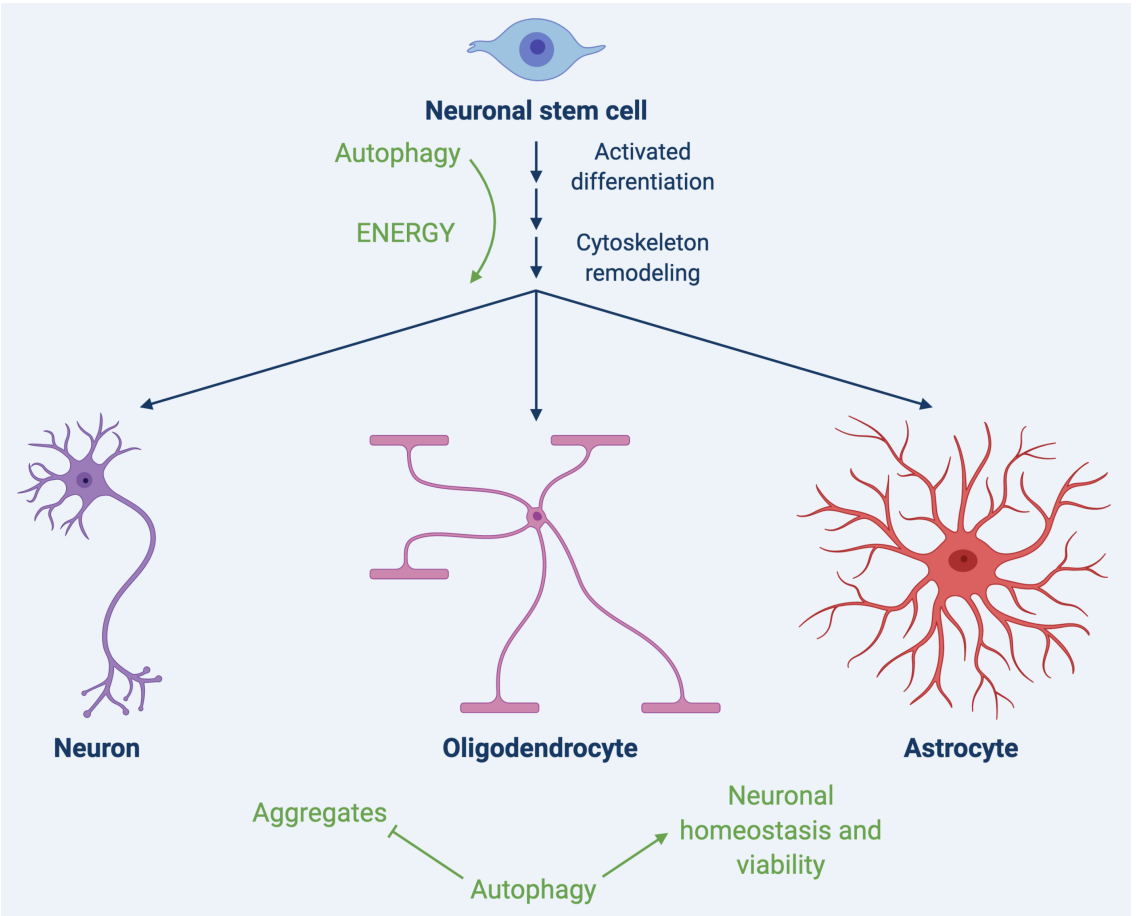

Figure 3

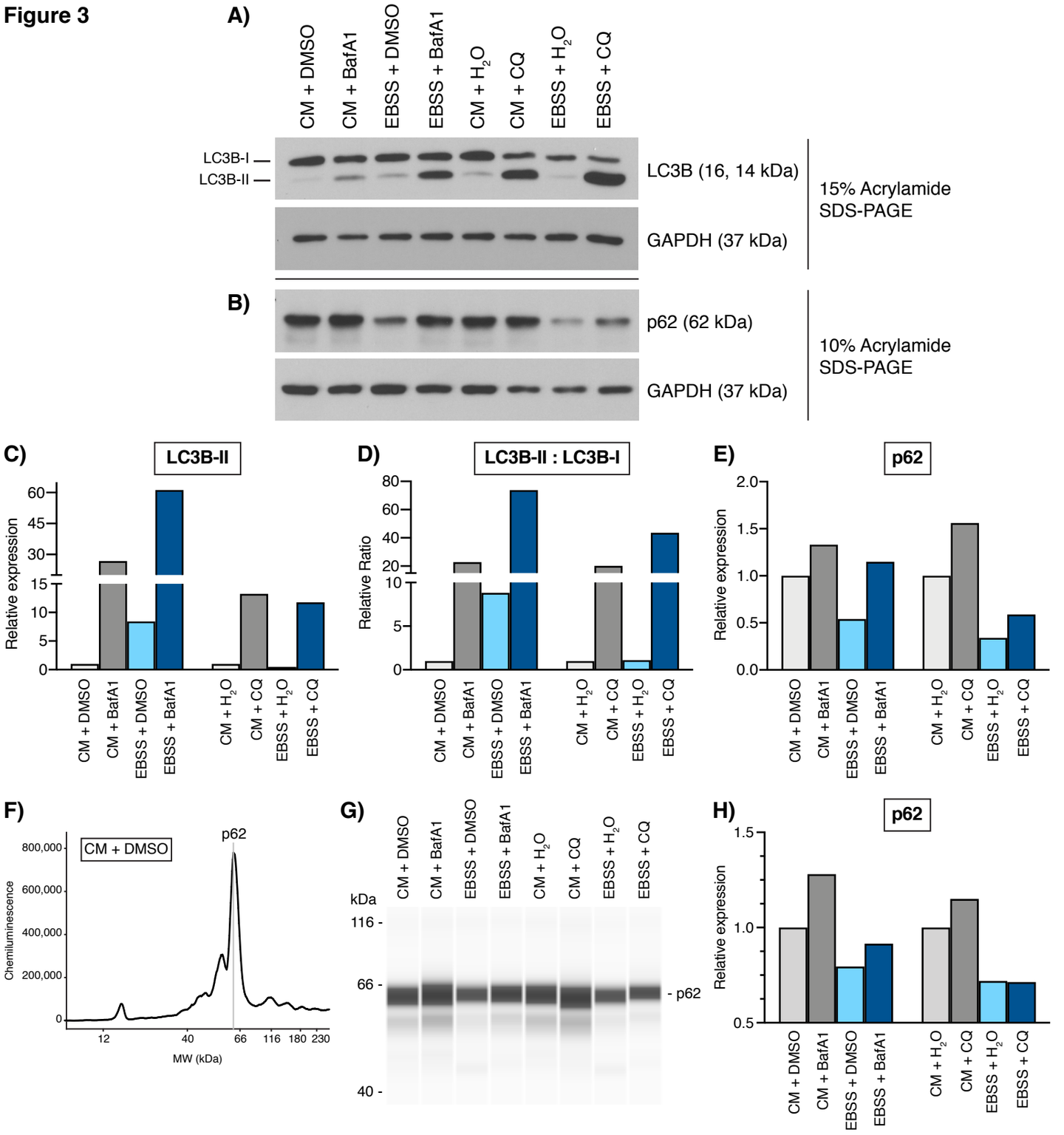
A)
CM + DMSO
CM + BafA1
EBSS + DMSO
EBSS + BafA1
CM + H2O
CM + CQ
EBSS + H2O
EBSS + CQ
LC3B-I
LC3B-II
LC3B (16, 14 kDa)
GAPDH (37 kDa)
15% Acrylamide SDS-PAGE
B)
p62 (62 kDa)
GAPDH (37 kDa)
10% Acrylamide SDS-PAGE
C)
LC3B-II
Relative expression
D)
LC3B-II : LC3B-I
Relative Ratio
E)
p62
Relative expression
F)
CM + DMSO
p62
Chemiluminescence
MW (kDa)
G)
kDa
116 -
66 -
40 -
- p62
H)
p62
Relative expression

Figure 4

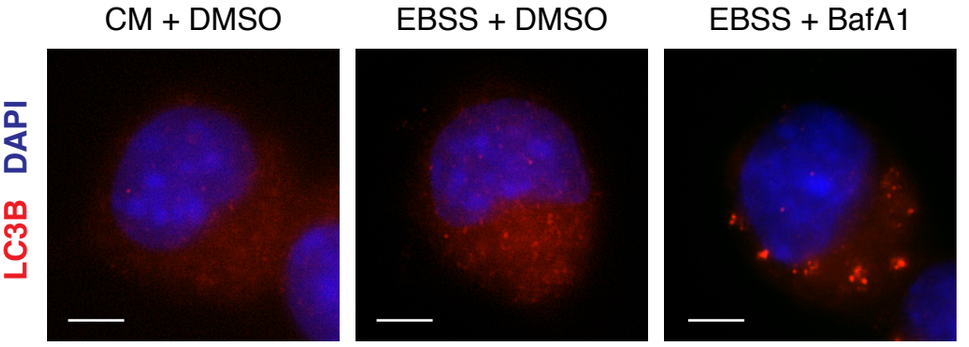

Figure 5